

# Closed porosity aluminosilicate for electronic packaging applications

S. L. Hietala and D. M. Smith

UNM/NSF Center for Micro-Engineered Ceramics, University of New Mexico, Albuquerque, New Mexico 87131-6041

V. M. Hietala and C. J. Brinker

Sandia National Laboratories, Albuquerque, New Mexico 87185

(Received 29 June 1992; accepted 30 December 1992)

The electrical properties of sol-gel prepared aluminosilicate films were investigated for suitability in electronic applications. The aluminosilicate films exhibited apparent closed porosity and a dielectric constant as low as  $\approx 5$  with processing temperatures from 373 K to 873 K. The porosity was inaccessible to nitrogen at 77 K, helium at 293 K, and water vapor at 293 K. Both bulk and thin-film samples were analyzed for hydroxyl and carbon contents to elucidate the relative dependence of the measured electrical properties on processing conditions. Experiments indicate it is possible to vary the porosity in bulk material in ways that should improve electrical properties.

## I. INTRODUCTION

Aluminosilicate xerogels prepared by sol-gel methods typically have nitrogen surface areas  $>100 \text{ m}^2/\text{g}$  (as do most sol-gel derived materials). A bulk aluminosilicate of composition 1:1 molar ratio of Al:Si exhibited an anomalously low surface area of  $<1 \text{ m}^2/\text{g}$  when prepared by a variety of sol-gel routes.<sup>1-3</sup> The surface area and skeletal density of the 1:1 material are compared in Fig. 1 with other similarly prepared aluminosilicate compositions. The dramatic decrease in surface area and density has been attributed to closed porosity, and from helium displacement measurements of the skeletal densities, closed porosities of 15% to 20% are calculated for the 1:1 composition. Films prepared from this material exhibited BET surface area of  $\approx 1 \text{ cm}^2/\text{cm}^2$  (accessible surface area per area of film), as measured using a surface acoustic wave (SAW) technique.<sup>4,5</sup> The unique property of a closed cell ceramic material, which can be obtained at low processing temperatures (373 K to 873 K), suggests uses in electronics packaging applications, as a result of its low gas/vapor permeability and conceivably low dielectric constant. Electrical and physical properties were measured as a function of heat treatment atmosphere, time, and temperature, and the effect on these properties due to the carbon and hydroxyl content in the films was determined.

## II. EXPERIMENTAL

The bulk and film materials were prepared using alkoxide precursors (as described previously).<sup>3</sup> Ethanol was added to tetraethylorthosilicate (TEOS) in a round bottom flask. A solution of ethanol and HCl (molar

ratios 1 EtOH: 1 HCl: 0.8 TEOS) was added to the flask, and then the aluminum tri-sec butoxide was mixed with this solution. This was allowed to react (with slight agitation) for several minutes, then diluted with ethanol to form a solution of 2 wt. % solids, and refluxed at 353 K overnight. A gel was formed by adding water (molar ratios 100  $\text{H}_2\text{O}:\text{Si}$ ) to the sol, with the gel time  $t_g \approx 4 \text{ h}$  at 298 K. To form a bulk powder, the gel was allowed to dry at room temperature for several days. The film sample was prepared by spin coating a 4 in. silicon wafer at 2000 rpm with the same sol at  $t/t_{\text{gel}} \approx 0.5$ . A relatively uniform coating was indicated by the wafer color, which turned a dark blue after heating. The wafer was then sectioned into pieces for each of the different heating procedures described below.

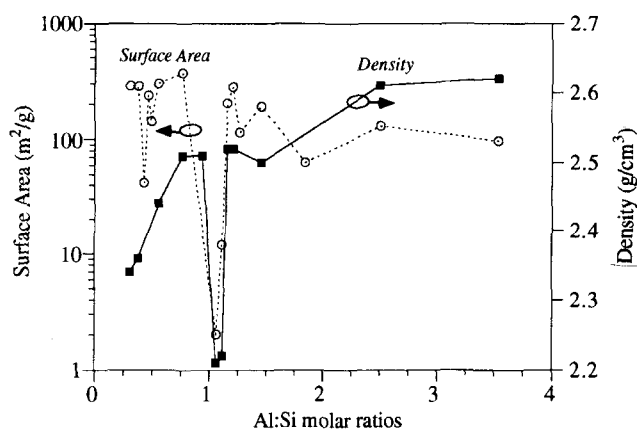


FIG. 1. Surface area and density of bulk aluminosilicates prepared by a sol-gel method (aluminum nitrate used as a precursor).<sup>1</sup>

Bulk and film samples were heated in a Lindberg quartz-tube furnace up to a preset temperature in the range of 373 K to 873 K, held for 2 h, then ramped down to room temperature. An additional set of films was held for 48 h before ramping down. The bulk samples were heated with a flow of air at a ramp rate of 2 to 10 K/min. The film samples were heated in a flow of air or nitrogen at a ramp rate of 2 K/min.

The film thicknesses were measured with an automatic ellipsometer (Rudolph AutoEL III, Rudolph Research, Fairfield, NJ 07006) using HeNe laser illumination (632.8 nm) at an incident angle of 70°. Several thickness measurements were made across the samples with typical variations of  $\approx 3\%$ . These variations are primarily due to an unbalanced load during spin coating.

The dielectric constants of the thin films were measured using a mercury probe. The technique (commonly used in the microelectronics industry for measuring thin-film insulator and semiconductor properties) involves applying two close-proximity drops of mercury in a very controlled manner to the sample surface. The large surface area of one drop, compared with that of the other, effectively forms a ground connection for the measurement. The smaller mercury drop forms a simple parallel plate test capacitor. The silicon wafer used was selected to have a very high doping level ( $N_d \approx 10^{19} \text{ cm}^{-3}$ , resistivity 0.008–0.020  $\Omega \text{ cm}$ ) in order to avoid the formation of a depletion layer within the silicon; additionally, a small positive bias (1 V) was used to cause accumulation in the semiconductor layer. No electric field dependence was found in the dielectric constant or quality factor measurements. The capacitance ( $C$ ) was measured using an HP4275A multifrequency LCR meter calibrated at the mercury probe. Since the area of the drop is accurately known ( $A = 2.03 \times 10^{-7} \text{ m}^2$ , at a constant vacuum of 6 mm Hg) and the film thickness can be easily measured by ellipsometry ( $t$  varied from 1119 Å to 2154 Å, depending on the sample), the dielectric constant can be easily determined from the parallel plate capacitor formula ( $k' = Ct/\epsilon_0 A$ ). The results from this technique agreed well with those obtained from the metal-insulator-metal test capacitor fabricated from evaporated aluminum.

Error sources in this technique arise from an uncertainty in the mercury drop's area and in an uncertainty in the film's thickness at the exact spot where the mercury makes contact. Absolute error of the measurement is estimated to be under 10% with the systematic error being significantly less.

Carbon content of the bulk material was measured by LECO Inc. using a LECO<sup>TM</sup> CS444 analyzer. Sample sizes of  $\approx 0.3 \text{ g}$  were analyzed in a 528-018 preheated crucible with  $\approx 1 \text{ g}$  Lecocel II (502-173) +  $\approx 1 \text{ g}$  iron chip (501-673) in a carrier gas of oxygen, with an analysis time of  $\approx 2 \text{ min}$ . The standard was a NIST

Standard Reference Material: 13 g with 0.613% carbon. Elemental analyses of the films were performed at Sandia National Laboratories using Auger spectroscopy, with a detection limit of 1 at. % for carbon.

Hydroxyl content of the bulk material was measured in a KBr pellet using a Mattson Instruments 6020 Galaxy Series FTIR (Mattson Instruments, Madison, WI). Hydroxyl content of the films was measured by reflectance IR using a BioRad 3200 S-40 FTIR at a reflectance angle of 60°. The samples were kept in a nitrogen atmosphere during the experiments.

Surface areas of the bulk powders were measured using nitrogen adsorption at 77 K, and five relative pressures in the range of 0.05 to 0.35 using an Autosorb-1 adsorption analyzer. Samples were outgassed under vacuum at 383 K (or lowest processing temperature) for 3 to 24 h before analysis. Surface areas were calculated using the BET equation and a molecular cross-sectional area of 0.162 nm<sup>2</sup>. Skeletal densities of the bulk powders were measured via helium displacement at 298 K using a Quantachrome micropycnometer or AccuPyc 1330 pycnometer.

Water adsorption was performed on a homemade volumetric system at five relative pressures, with an equilibration time of 24 h per point at a temperature of 288 K. The cross-sectional area of the water molecule was 0.108 nm<sup>2</sup>. Due to the small volume-to-surface area of the sample, the errors associated with this technique may be quite high, so this may be regarded as a semi-quantitative technique for these samples.

### III. RESULTS AND DISCUSSION

Design of high-performance packages for high-speed circuits requires robust materials with relatively low dielectric constants for minimization of propagation delays of signals. Packaging materials should possess physical, chemical, and thermal stability, at least as effective as the inorganic materials now widely used, including epoxy-glass and glass-bonded alumina among others. The material should also be easily synthesized and applied, as in sol-gel prepared materials. A study by Yarbrough *et al.* investigated sol-gel prepared colloidal silica for such a packaging material.<sup>6</sup> Although the films exhibited low dielectric, and otherwise good electrical properties, the material was processed at high temperatures (1173 K to 1273 K) and exhibited open porosity. A more versatile material would be one that can be processed at low temperatures, and provides an impermeable barrier, while exhibiting a low dielectric constant. The 1:1 aluminosilicate composition with its closed porosity should exhibit such properties. The range of porosity (15% to 20%) was calculated for the bulk powders and films from density and ellipsometry data. Figure 2 shows a theoretical plot of the dielectric constant as a

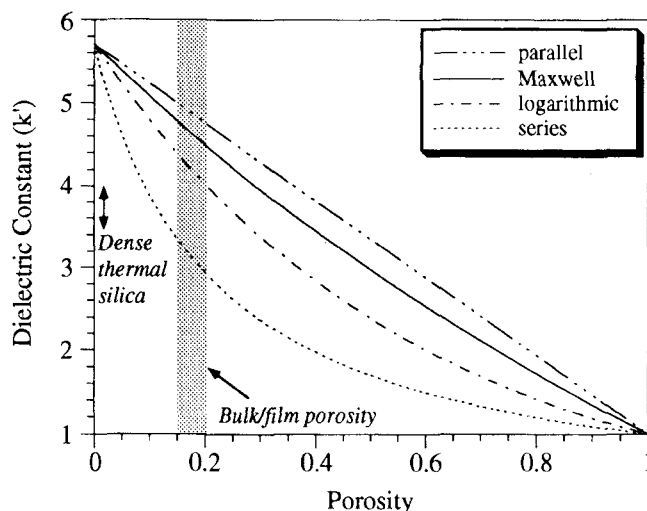


FIG. 2. Theoretical dielectric constant as a function of porosity in a 1:1 composition aluminosilicate.

function of porosity of a 1:1 composition film. Theoretical curves were generated assuming a homogeneous mixture of  $\gamma$ -alumina ( $k' = 9.3$ ) and amorphous silica ( $k' = 3.9$ ), obtaining the value of  $k'_{\text{aluminosilicate}} = 5.7$ , with the porosity computed as a separate phase from the aluminosilicate.<sup>7</sup> Four models commonly used in an attempt to describe these composite dielectric properties include the series and parallel models, where layers of the phases are assumed to be either perpendicular or parallel to the applied field, respectively, the Maxwell model derived for small spherical inclusion in a continuous matrix, and the logarithmic model for materials with intermediate connectivity or irregularly shaped inclusions. Figure 2 shows that in the porosity range of the bulk and thin film specimens, the theoretical relative permittivities range from 2.8 (series model) to 5.0 (parallel model).<sup>7</sup>

For predominantly electronic solids such as diamond, polymers, crystals, and glasses, the dielectric constant is closely related to the optical index<sup>8,9</sup>:

$$k' \propto n^2 \quad (1)$$

From the measured optical index ( $n \approx 1.53$  at 873 K), if this were crystalline or glassy (with no other active contributions), we would expect a dielectric constant of  $\approx 2.3$ . There may be, however, contributions to the overall dielectric constant from different polarization mechanisms related to composition, frequency, and temperature.<sup>8</sup>

The dielectric constant of thin films as a function of temperature and heating atmosphere (measured at 100 kHz) is shown in Fig. 3, along with the values remeasured after one year. There is a large decrease from the material as-spun and dried at room temperature compared with those heated to higher temperatures. The

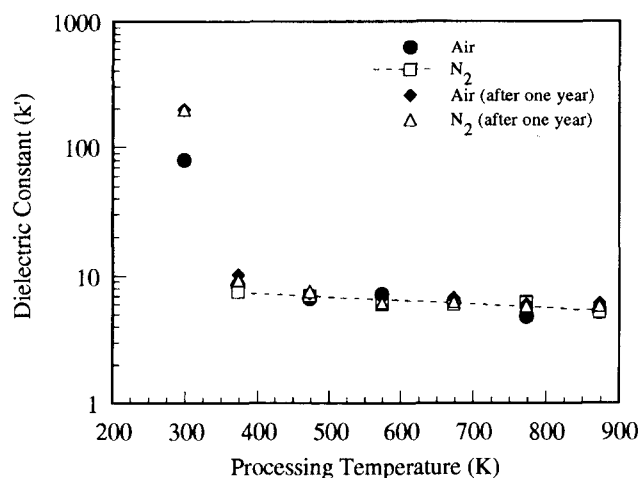


FIG. 3. Dielectric constant of the aluminosilicate films as a function of processing temperature and heating atmosphere. Original measurements and those taken after one year.

different atmospheres had relatively little effect on the dielectric constant compared to the temperature and time factors. From 373 K to 873 K, the dielectric constant decreased in a roughly exponential fashion from  $k' \approx 9$  to  $k' \approx 5$ .

Figure 4 shows the frequency dependence of the dielectric constant and compares film samples heated for 2 h with those heated for 48 h. In the 373 K sample heated for 2 h, there is an apparent dipole polarization occurring at low frequencies as seen by the rapid decrease in the dielectric constant at higher frequencies. No loss peak was observed in the measurements at that resolution, although the relative loss factor ( $k'' = k'/Q$ ) plotted against the frequency had the form of the tail-end of a Gaussian curve. This was not evident in the sample heated for 48 h. This is most likely due to the chlorine, which was used as a catalyst in the sol-gel synthesis, and

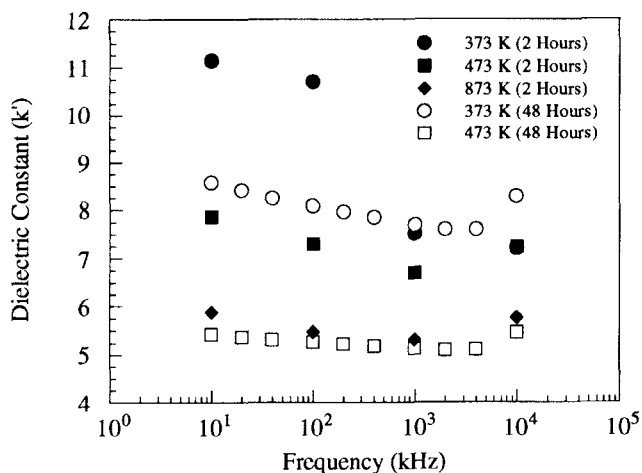


FIG. 4. Frequency dependence of the dielectric constant of aluminosilicate films that had been heated for 2 h or 48 h.

found only in small amounts in the 373 K (2 h) film. The lowest dielectric constant obtained is still above the theoretical value of 2.2 derived from the optical index measurements. However, it is evident from the IR studies that there are still some hydroxyl contributions, even at 873 K.

The large decrease in thickness, between 298 K and 473 K in Fig. 5, is probably the result of continued condensation reactions and pore collapse. In Fig. 6, this is shown as an increase in the optical index, or a decrease in the porosity of the films. The optical index,  $n$ , originally had unusual behavior by peaking at midrange temperatures (473 K to 673 K), but this trend was not seen in the measurements after the films had aged for one year. The adsorbed water on the unheated samples causes an unusually low optical index at low temperatures, and as the samples are heated, the water desorbs, which may cause changes in the pore structure due to capillary forces and condensation of surface  $-OH$  groups, as discussed for the thickness measurements.<sup>10</sup> The chemisorbed water is expected to be driven off by 673 K. The optical indexes of nonporous, homogeneously mixed aluminosilicates ( $\gamma$ -alumina and amorphous silica) range from 1.52 to 1.55.<sup>6</sup>

The quality factor (Fig. 7) increases with increasing temperature and time. The quality factor is a measure of the losses in the film and is found by  $1/(\text{loss tangent})$ .<sup>8,11-13</sup>

$$Q = \frac{1}{\tan \delta} = \frac{\text{average energy stored}}{\text{energy dissipated per cycle}} = \frac{k'}{k''} \quad (2)$$

where  $Q$  is the quality factor  
 $\tan \delta$  is the loss tangent  
 $k'$  is the dielectric constant  
 $k''$  is the relative loss factor.

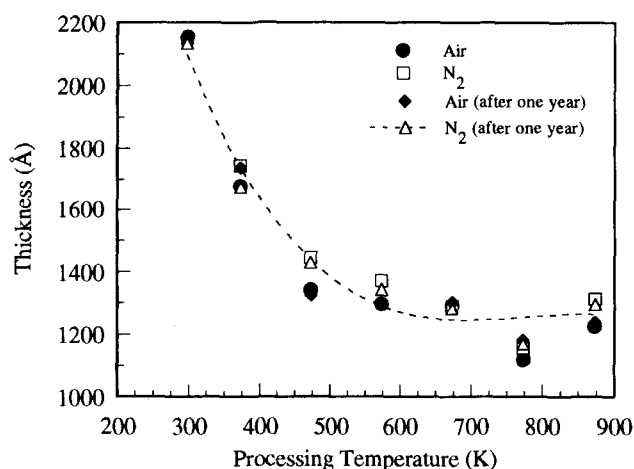


FIG. 5. Aluminosilicate film thickness as a function of heat treatment, temperature, and atmosphere.

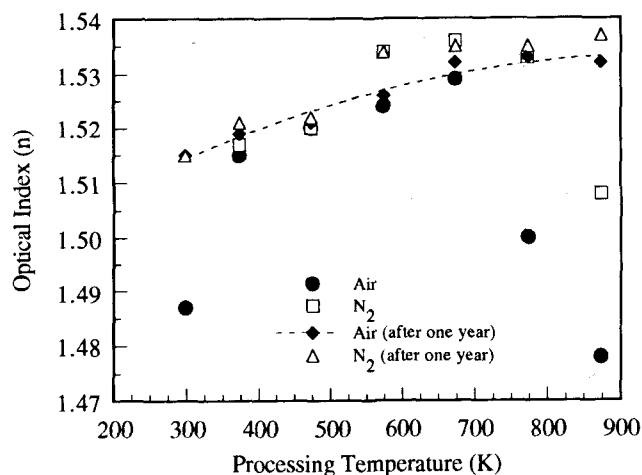


FIG. 6. Optical index of aluminosilicate films as a function of film heat treatment in various atmospheres.

The dissipation factor represents the relative expenditure of energy to obtain a given amount of charge storage in a cycle. The quality factor can be maximized by a small dielectric constant or a low loss angle. The relatively low quality factors, especially at low temperatures, could be due to the hydroxyl content in the films.

The carbon content of the bulk material is shown in Table I. The majority of the carbon in the materials (at least in the bulk, and presumably in the films as well) burns out by 673 K. Previous investigators have shown that increasing carbon content in silicate films increases the dielectric constant.<sup>14</sup> None of the electronic properties shown in Figs. 3 through 7 shows any anomalous behavior in this region where the dramatic drop in carbon content appears. Therefore, the carbon content in these films is found to have little effect on the electronic properties.

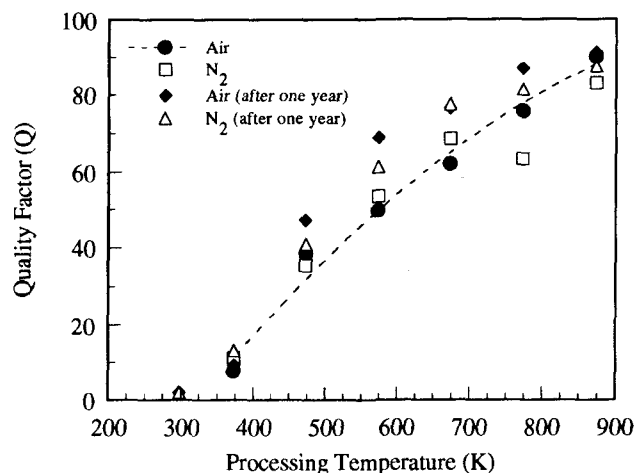


FIG. 7. Quality factor (1/loss tangent) of aluminosilicate films as a function of heat treatment and atmosphere.

TABLE I. Percent carbon in bulk samples at various heat treatments.

Heat treatment temp. (K)	% carbon
298	0.61
373	0.91
473	0.67
573	0.75
673	0.19
773	0.19
873	0.27

The hydroxyl content, however, strongly contributes to the electronic properties of the films. The hydroxyl content of the films was measured semiquantitatively by reflectance IR,<sup>15</sup> with the results tabulated in Table II. Reflectance IR can be relatively difficult to interpret due to interference fringing, changes in the optical index, or thick films requiring the use of the Kramer-Kronig relationship (which takes into account the optical index of the sample) for samples in which the front surface dominates the signal.<sup>16</sup> Because the films were relatively thin, the signal was dominated by reflectance/absorption interactions, which gave spectra very close to that which would be obtained in transmission IR. To obtain relative ratios of the hydroxyl content in the films, the regions between 2700 and 3740, encompassing the hydroxyl region of the spectrum, were integrated. The ratio of these numbers to that of the unheated films (298 K) was calculated. The results show a steady decrease in the hydroxyl content of the films with increasing temperatures, as did the TGA and IR results from the bulk powders.

The frequency of the Si-O peak (1000 to 1400  $\text{cm}^{-1}$ ) shifted slightly from the unheated sample peak at 1180 to the sample heated to 873 K, peaking at about 1220  $\text{cm}^{-1}$ . This may be due to film stiffening through continued condensation reactions, consistent with the thickness and optical index results.

The monotonic decrease in the hydroxyl content with increasing heat treatment temperatures relates well to the decrease in dielectric constant and the increase in quality factor. The structure of gels may be significantly

TABLE II. Relative -OH ratios in films heated in air or nitrogen.

Temp. (K)	Ratio of -OH peak area to 298 K: air	Ratio of -OH peak area to 298 K: N <sub>2</sub>
298	1	1
373	0.95	0.94
473	0.69	0.62
573	0.61	0.50
673	0.59	0.48
773	0.46	0.43
873	0.36	0.38

altered by aging under various processing conditions (temperature, time, pH, and solvent) before drying.<sup>17</sup> Aging at higher pH should result in increased dissolution/precipitation, and, hence, a stiffer gel that will not collapse as severely during drying. This suggests a scheme for increasing porosity and decreasing the dielectric constant. For bulk 1:1 composition aluminosilicate samples, this is illustrated in Fig. 8 as porosity (deduced from skeletal densities) versus pH of the aging fluid and aging time. Although there is some experimental scatter, a trend of increased total closed porosity versus increased aging pH is clearly seen.

Table III shows water adsorption data for the bulk materials. Relatively little water adsorption occurs, even at high relative pressures. The initial two adsorption uptakes are similar, and are not distinguishably different due to the small sample size. Based on the initial surface area of 0.8  $\text{m}^2/\text{g}$ , the lowest adsorption relates to approximately one monolayer of water adsorption, while the highest is approximately three monolayers. This indicates essentially no water is penetrating pores that are inaccessible to nitrogen at 77 K, or a much larger increase would be seen when the water accessed the 15% closed porosity.

Table IV lists the properties of some microelectronic packaging materials currently used, and makes comparisons with those of the aluminosilicate discussed in this paper. The electronic properties of the aluminosilicate, even now, seem well within the range of those currently used; additionally, the closed porosity of the material makes it an attractive packaging alternative. The properties measured after a period of one year were nearly identical to the original measured values, indicating stability of the films, especially against adsorbing water. The residual hydroxyl content and decreasing porosity with increasing temperature must be further studied. If

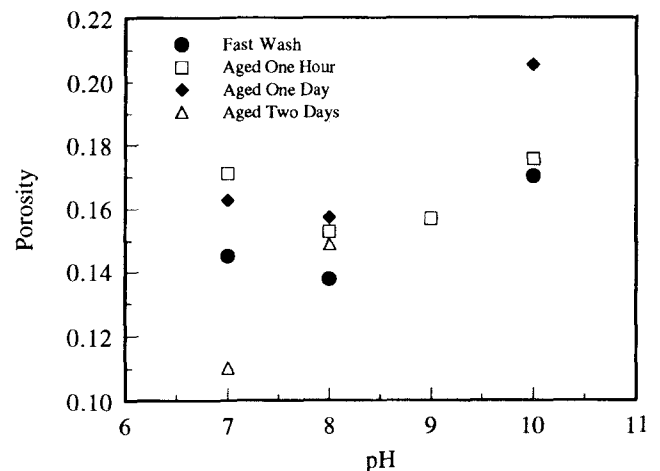


FIG. 8. Porosity in bulk aluminosilicate powders after aging for various times at different pH values.

TABLE III. Water adsorption of 1:1 composition aluminosilicate bulk powders.

$P/P_0$	Weight adsorption (g/g)
0.163	0.0045
0.232	0.0045
0.500	0.0060
0.836	0.0090

the hydroxyls could be eliminated in the closed pores, a much lower dielectric constant could be achieved. In addition, studies of the bulk material indicate it is possible to tailor the porosity of the material, which may further enhance the electronic properties as well as indicate a way to maintain porosity at higher temperatures.

### ACKNOWLEDGMENTS

We would like to thank Srinu Sundararajan, Ross Thomas, Dr. Richard Crooks, Dr. David Haaland, and Dr. Herb Tardy for assistance and discussions of the IR measurements. We would also like to thank Greg Johnston for the water adsorption measurements, and Bill Ackerman for the bulk surface area and density measurements. Work performed at Sandia National Laboratories was supported by the United States Department of Energy under Contract No. DE-AC04-76P00789.

TABLE IV. Properties of microelectronic packaging materials.<sup>18</sup>

Material	Process temp. (K)	Dielectric constant
Polyimide	573– 623	3– 4
Epoxy-glass	423– 473	4– 5
Glass-ceramic	1123–1273	6– 8
Alumina	413–1873	9–11
Alumina-fiber/polyimide	573– 623	4.5– 6.5
AlN-fiber/teflon	573– 623	2.8– 5
Aluminosilicate	373– 873	5– 9

### REFERENCES

1. S. L. Hietala, J. L. Golden, D. M. Smith, and C. J. Brinker, *J. Am. Ceram. Soc.* **72**, C2354 (1989).
2. S. L. Hietala and D. M. Smith, "Low Density/Low Surface Area Silica-Alumina Composition," patent SN 5 028 352, July 2, 1991.
3. S. L. Hietala, D. M. Smith, C. J. Brinker, A. J. Hurd, N. Dando, and A. H. Carim, *J. Am. Ceram. Soc.* **73**, 2815 (1990).
4. S. L. Hietala, D. M. Smith, V. M. Hietala, G. C. Frye, A. J. Hurd, and C. J. Brinker, in *Better Ceramics Through Chemistry IV*, edited by B. J. J. Zelinski, C. J. Brinker, D. E. Clark, and D. R. Ulrich (Mater. Res. Soc. Symp. Proc. **180**, Pittsburgh, PA, 1990), pp. 433–437.
5. C. L. Graves, G. C. Frye, D. M. Smith, C. J. Brinker, A. Datye, A. J. Ricco, and S. J. Martin, *Langmuir* **5**, 459 (1989).
6. W. A. Yarbrough, T. R. Gururaja, and L. E. Cross, *Am. Ceram. Soc. Bull.* **66** (4), 692 (1987).
7. *CRC Handbook of Chemistry and Physics*, 70th ed., edited by R. C. Weast (CRC Press Inc., Boca Raton, FL, 1989–1990).
8. W. D. Kingery, H. K. Bowman, and D. R. Uhlmann, *Introduction to Ceramics*, 2nd ed. (John Wiley & Sons, New York, 1976), Chap. 18.
9. R. C. Buchanan, *Ceramic Materials for Electronics: Processing, Properties and Applications* (Marcel Dekker, Inc., New York, 1986).
10. C. J. Brinker and G. W. Scherer, *Sol-Gel Science: The Physics and Chemistry of Sol-Gel Processing* (Academic Press, Inc., San Diego, CA, 1990), pp. 453–617.
11. *Dielectric Materials and Applications: Papers by 22 Contributors*, edited by A. R. von Hippel (John Wiley & Sons, New York, 1954).
12. W. H. Hayt, Jr., *Engineering Electromagnetics*, 4th ed. (McGraw-Hill, Inc., New York, 1981).
13. L. L. Hench and J. K. West, *Principles of Electronic Ceramics* (John Wiley & Sons, Inc., New York, 1990).
14. G. V. Chandreshkhar and M. W. Shafer, in *Better Ceramics Through Chemistry II*, edited by C. J. Brinker, D. E. Clark, and D. R. Ulrich (Mater. Res. Soc. Symp. Proc. **73**, Pittsburgh, PA, 1986), pp. 705–710.
15. K. Nakamoto, *Infrared and Raman Spectra of Inorganic and Coordination Compounds*, 3rd ed. (John Wiley & Sons, New York, 1978).
16. C. Kittel, *Introduction to Solid State Physics*, 5th ed. (John Wiley & Sons, New York, 1976).
17. P. J. Davis, C. J. Brinker, and D. M. Smith, *J. Non-Cryst. Solids* **142**, 189 (1992).
18. *Ceramic Source* **6**, 329 (1990).